N69-33318
NASA CR-101134

INVESTIGATION OF THE KINETICS OF CRYSTALLIZATION OF MOLTEN BINARY AND TERNARY OXIDE SYSTEMS

H910373-15

by

James F. Bacon

AUGUST 1, 1969

United Aircraft Research Laboratories

UNITED AIRCRAFT CORPORATION

EAST HARTFORD, CONNECTICUT

QUARTERLY STATUS REPORT NO. 15

CONTRACT NASW-1301

United Aircraft Research Laboratories

UNITED AIRCRAFT CORPORATION

EAST HARTFORD, CONNECTICUT

Investigation of the Kinetics of Crystallization of
Molten Binary and Ternary Oxide Systems

Quarterly Status Report No. 15

Contract NASW-1301

REPORTED BY

J. F. Bacon

APPROVED BY M. A. De Crescente

M. A. DeCrescente, Chief
High Temperature Materials

DATE 8/1/69

NO. OF PAGES 30

COPY NO. ________

Investigation of the Kinetics of Crystallization of

Molten Binary and Ternary Oxide Systems

Quarterly Status Report No. 15

TABLE OF CONTENTS

Investigation of the Kinetics of Crystallization of

Molten Binary and Ternary Oxide Systems

Quarterly Status Report No. 15 - March 1, 1969 through June 30, 1969

Contract No. NASW-1301

SUMMARY

This report is based on the research studies carried out in the fifteenth quarter of Contract NASW-1301. In the last month the contractual period for this extension has been lengthened from nine to ten months so that the fifteenth quarter is actually four months, starting March 1, 1969 and extending to June 30, 1969. Thirty-two new glass compositions were conceived, prepared and partially characterized in this period. Similar characterization studies were completed for some of the compositions reported earlier and these include density, Young's modulus, and fiberizability determinations. In addition, one of the two commercial-type platinum-20% rhodium single hole glass fiber bushings has been installed and used to produce "E" glass for strength determinations on pristine fibers.

At the time of this report, a total of a dozen glass compositions have been developed with values for Young's modulus measured on bulk samples greater than twenty million pounds per square inch and another dozen have values for Young's modulus between nineteen and twenty million psi. The best of these appears to be an "invert" analog glass, UARL 383, with a Young's modulus of 22.75 million pounds per square inch, a specific modulus of 200 million inches, and with no toxic ingredients. The best data for the experimental glasses actually measured on fibers of that glass is a Young's modulus of 19.8 million pounds per square inch for UARL 331.

INTRODUCTION

This is the fifteenth quarterly report for Contract NASW-1301 entitled "Investigation of the Kinetics of Crystallization of Molten Binary and Ternary Oxide Systems". The fifteenth quarter started March 1, 1969 and due to a change in contractual terms, ended June 30, 1969 and forms the second quarter of the fourth ten month extension to the contract which runs from December 1, 1968 through September 30, 1969.

The primary objective of the contract is to gain a better understanding of the mechanisms of glass formation by measuring the rate at which crystallization occurs and the effect of antinucleating agents on the observed crystallization rate for systems which tend to form complex three-dimensional structures. The composition of the molten oxide systems selected for study, the reasons for their selection, and the methods used to prepare them form the first major section of this report. It will be noted that the report emphasizes those molten oxide systems that tend to form complex three-dimensional structures such as rings or interpenetrating layers since this approach, as will be shown, has resulted in several new glass compositions with increased values for Young's modulus.

The research, therefore, continues to emphasize the viewpoint that glass formation must be considered as a rate phenomenon and will continue to concentrate on systems that tend to form complex many-atom three-dimensional molecules and which have suitable viscosity and surface tension to permit mechanical drawing of glass fibers. This view of the glass formation process justifies the consideration of oxide systems previously thought impractical and allows the search for systems that may yield high-strength, high-modulus glass fibers to be carried out on an unusually broad basis.

Characterization of the experimental glasses produced as bulk specimens is the subject of the second major section of the report. Such characterization is primarily achieved by measuring the density and the value of Young's modulus for bulk samples of the experimental glasses. Originally, specimens for measuring Young's modulus on bulk glasses were prepared by casting a slab of the glass, annealing it, and then cutting rectangular bars from the slab with precision optical grinding equipment. Now, however, we form samples suitable for modulus determinations either by pulling molten glass into coated (magnesia) fused silica tubes by means of controlled suction supplied by a hypodermic syringe or by casting rods to prerequisite shape in a preheated graphite mold. Consequently, measurements of Young's modulus are much less costly to make.

Observations on the fiberizability of the various melts including the first use of the new UARL commercial type platinum-20% rhodium single hole bushing form the final major section of the report. This section also includes the attempts to make strength measurements on pristine fibers of "E" glass produced with the UARL bushing.

SELECTION AND PREPARATION OF GLASS SYSTEMS FOR PRELIMINARY EVALUATION

Our earlier reports (UARL H910373-13 and UARL H910373-14) have stressed the fact that the glass systems we normally investigate must consist primarily of low atomic number oxides but not exclusively so, since the rare earths and zirconia make a sufficiently large molar contribution to Young's modulus to allow their inclusion as well. We have also repeatedly mentioned in these same and earlier reports that favored proportions of these low atomic number oxides are those proportions that tend to form complex three-dimensional molecules such as cordierite, beryl, or benitoite and we continued to follow these considerations for approximately half of the new compositions originated in this quarter. The cordierite-rare earth glass systems had given values for Young's modulus up to 20.9 million psi and the beryl-cordierite-rare earth systems had an even higher value of 21.1 million psi for Young's modulus and a specific modulus of 174.5 million inches.

The other half of the new compositions tried in this quarter belong to the glass composition field of UARL "invert" analog glasses (UARL H910373-13 and UARL H910373-14) since these kinds of compositions had been found to give values for Young's modulus as high or higher than the cordierite-rare earth glass systems. However, instead of the direct frontal attack on these two areas of compositions characteristic of many of our recent reports (UARL G910373-10 through UARL H910373-14), we have attempted to modify these two glass composition fields in accordance with the rules and observations gained from the published literature and summarized in UARL H910373-13, in the section called "Compositional Changes to Improved Workability of 'Invert' Glasses". The primary aim of this work has been to lower or raise viscosity of a given composition, to increase the working range of a glass in question, to raise or lower its surface tension, and in general to increase the ease with which glass fibers can be mechanically drawn at high speed from the glass under investigation.

The compositions for the modified glasses originated subject to these considerations are shown in terms of grams of actual ingredient in Table I. Since only a small number of the modifications to be evaluated have been tried as yet we shall not draw any conclusions except for the effect of the one ingredient, fused boric oxide. From the section in UARL H910373-13 referred to in the above paragraph, the effects expected when fused boric oxide is included in the ingredients are an increase in stability of glass and a decrease in devitrification tendency, perhaps a very slight or no increase in modulus, a decrease in liquidus and viscosity for silica-base glasses but possibly an increase in viscosity and a decrease in liquidus for "invert" analog glasses, and a marked decrease in density with corresponding increase in specific modulus.

The glasses of Table I having a significant amount of boric oxide content are separated to form Table II and the compositions expressed in mol % in place of actual grams of ingredients. Table II also lists the density if measured at this time, Young's modulus, specific modulus and molal sum. It is immediately apparent that, in general, the values for Young's modulus for these glasses are inferior to many other glasses developed at UARL (cf. Table III) while the specific modulus is not markedly increased. In addition, these glasses do not fiberize readily. Two exceptions to these general remarks are UARL 382 and 383. UARL 383, in particular, is the highest modulus glass yet developed and has the highest specific modulus but attempts to fiberize this glass have been unsuccessful to date. Work toward a more complete understanding of the results found for UARL 383 is in progress. Another factor encountered in the study of the glasses with appreciable borate content is that the addition of beryllia to such glasses (for example, UARL 387 and 388) does not raise Young's modulus as much as does the addition of beryllia to a silica-alumina-magnesia glass.

Once compounded the glasses of Tables I and II were prepared in the usual manner by melting 500 gram batches of the specified raw materials in high purity alumina crucibles in air using kilns heated by Super-kanthal hairpin electrical resistance elements. All starting materials were of reagent grade to facilitate interpretation of results and were mixed by being ball-milled together for twenty-four hours. The handling of the somewhat flocculent raw materials was made easier by forming pellets of the materials using a hydraulic press and dies. These pellets also formed an easy way to introduce additions into the hot crucibles since they could be slid down a large diameter silica tubing directly into the crucible while it remained in the kiln.

CHARACTERIZATION OF UARL EXPERIMENTAL GLASSES

In the earlier reports of this program, for example UARL H910373-13, the methods employed for determining the density and Young's modulus on bulk samples are discussed in detail. In this quarter the same procedures were followed to obtain the values tabulated. In Table III, the values of density and Young's modulus for the experimental glasses that had been measured prior to this quarter are summarized for comparative purposes while in Table IV the new data obtained in the fifteenth quarter is entered. In table V the data for the best glasses obtained to date in the cordierite-rare earth systems and the beryl-cordierite rare earth systems has been made more readily available and in Table VI a like summary for the UARL "invert" analog glass systems is given. It will be noted that values as high as 22 3/4 million psi for Young's modulus and 200 million inches for specific modulus occur. Additional test data not summarized in this report show that mechanically drawn fibers of several of these glasses have correspondingly high values for Young's modulus although these values are customarily 1/2 to one million psi lower than the bulk glass from which they are derived.

Estimation of Liquidus and Working Range

Other important quantities for any new glass are its liquidus and working range and these are directly measured and estimated by means of the UARL microfurnace. This microfurnace is based on the design of an earlier furnace constructed by Morley (Ref. 1) for the study of crystallization kinetics in molten glass. It consists primarily of a platinum-20% rhodium tube, 0.250 in. O.D. and with a wall thickness of 3 mils which is clamped between the copper bars (0.187 in. x 0.750 in.). A circular shelf of platinum is welded to the inside of the tube and the crucible is placed in a 1/8 in. hole in this shelf. Crucibles are fabricated by cutting platinum tubing (1/8 in. diameter with a 5 mil wall thickness) into pieces 1/16 in. long and then pressing them in a die so that they form a 40 degree included angle.

Figure 1 shows the microfurnace without its usual radiation shielding. When used, however, radiation shielding is added by welding two rings of 0.057 kanthal wire to the nichrome plates at the two ends of the heater tube and then welding an inner shield of 4 mil platinum-rhodium sheet and an outer shield of 5 mil nichrome sheet to the inner nichrome wire ring on the lower nichrome plate. Two 5 mil nichrome shields are also welded to the outer nichrome wire ring on the upper circular nichrome plate. Figure 1 also shows the 1/8 in. diameter copper tubing which is used to supply water cooling to the copper, electrical connections. The power supplied the furnace is from a filament transformer of 1 KVA nominal rating and is controlled by a twenty ampere rating Variac. Temperatures of 1400°C require only a current of 140 amperes at 1.1 volts 60 cycle a.c.

The complete experimental arrangement, but not including the power supply, is shown in Fig. 2 and comprises the microfurnace, microscope and camera, micromanipulator for welding and positioning the thermocouple, the x-y recorder used for plotting time-temperature response of the furnace, and the 3 mil platinum-platinum 10% rhodium thermocouple accurately positioned in the center of the furnace. Laboratory experience indicates that the furnace temperature can be maintained to $\pm$ 5°C at 1250°C.

For actual observations of liquidus and working range of an experimental glass, the crucible is placed in the furnace, a large fragment of glass placed in the crucible, and the crucible then heated. Smaller glass fragments are later added to completely fill the crucible. The glass is then heated until all of the bubbles disappear, cooled to the temperature selected for observation, and the thermocouple is then lowered into the melt. The glass is next heated until homogenized by convection currents and then cooled to allow crystals to nucleate and grow to a few tens of microns in diameter. The crucible is then reheated until the crystals disappear, the temperature noted and the process repeated until a consistent liquidus temperature is obtained. The viscosities of the experimental glasses are estimated by comparing their behavior when stirred with the thermocouple against the mental image retained from prior similar experiments with "E" glass. It must be clearly realized, therefore, that the temperatures we tabulate for such viscosity estimates are subjective temperatures.

The data collected from many of the experimental glasses is shown in Table VII. For some of the missing glass numbers in the range of the current tests, UARL 333 through UARL 377, only partial data could be obtained or the liquidus was too high for range of operation of the microfurnace or the glass too strongly absorbing to permit such visual observations. The significance of the data obtained can be seen from the fact that UARL 370, 371 and 372 proved very suitable for mechanically drawn fibers.

FIRST ATTEMPTS TO MEASURE STRENGTH ON FIBERS FORMED USING COMMERCIAL FORM SINGLE HOLE BUSHING

The "poor-man's bushing" in use at UARL in the earlier months of this contract and described in detail in several of our reports, F910373-7, F910373-8, F910373-9 and G910373-10, failed to yield sufficiently uniform and defect-free fiber suitable for strength measurements. UARL has, therefore, purchased two platinum-20% rhodium single hole glass bushings of the more conventional type as shown in Fig. 3. This design, which is a UARL design, hopefully combines the best features of single-hole bushings described by Tiede (Refs. 2,3) and the National Bureau of Standards (Ref. 4). The two bushings have now been tested and installed and one of these was used to form large amounts of "E" glass fiber for the strength measurements described below.

Because of the sensitivity of glass fiber to surface damage that can result from winding it on a drum or any similar contact, and by exposure to uncontrolled atmosphere for even very short times, it has become the practice to report so-called "virgin strength" of freshly drawn glass fiber. This is accomplished by capturing a sample of the fiber between the bushing and the winding drum, and measuring the tensile strength as quickly as possible before any obvious damage has occurred. In capturing the test specimen, a paper tab fiber mounting system has proven desirable because such a system provides a degree of self-alignment for the tensile specimens, and the paper mounts help absorb the energy of the fiber whiplash thus damping fly-out. Further, such a system makes possible the preparation of several tensile specimens from each captured fiber. The capture device is made long enough to engage eighteen-inch lengths of fiber between the bushing and the take-up spool and Fig. 4 shows the device mounted on the fiberization furnace. The captured fiber is picked off the capture device using a bent wire frame to which the fiber is temporarily glued, and transferred to a precut paper tape consisting of five paper mounting tabs, and then attached to the tabs using de Khotinsky cement applied with a pencil-sized soldering iron. The tensile specimen is then cut from the tape and mounted on the testing machine.

The fiber testing machine used to evaluate the captured paper-mounted tensile specimen is shown in Fig. 5. This machine was developed at UARL and has been described in the literature (Ref. 5). The fiber is mounted between the moving cross head (A) and the stationary cross head. The cross head moves at a constant rate of 0.77 mm/min. The load cell, which is mounted on the stationary cross head is of the strain gage type and is temperature compensated and so designed as to respond only to load components in the direction of the fiber axis. An electronic bridge circuit monitors the load cell, which is calibrated by placing the test device in the vertical position and suspending laboratory weights from the load cell. A calibration curve for the load cell relates the dial reading to the load in pounds.

In Fig. 6 the tensile specimen, together with its paper tab, is shown in position on the testing machine. It is actually mounted using spring clips and the mounting tab cut so as to permit loading the fiber.

The "E" glass used in this experiment was prepared by remelting the commercial "E" glass marbles to obtain a slug which fit the single-hole bushing chamber. This slug was then carefully degreased, washed in alcohol, rinsed in distilled water, and placed in the bushing. The bushing was then heated to the appropriate temperature and fibers drawn at the maximum rate than obtainable with the mechanically driven winder, at a speed of about 4000 ft/min. Twenty strength samples were snatched using the procedures outlined in the preceding paragraphs, each long sample furnishing five smaller samples on which the actual measurements were made. The results of these hundred strength determinations are entered in Table VIII. It will be immediately noted that the results are highly discordant, that no results in general as high as the average of 530,000 psi usually reported for "E" glass fibers (Ref. 6) were found, but instead typically very low strengths of 150,000 to 200,000 psi were measured. It is evident that we must make further improvements in measuring strength and these are in progress.

CONCLUSIONS

1. The UARL "invert" analog glass system has yielded glasses with a bulk value for Young's modulus of 22 3/4 million psi and a specific modulus of 200 million inches.

2. The cordierite-rare earth glass has produced glasses with bulk values for Young's modulus of 21.1 million psi and a specific moduli of 174 million in.

3. Attempts to increase the specific modulus and improve the working characteristics of the UARL experimental glasses through the addition of fused boric oxide to the ingredients have been only partially successful as yet.

4. The best experimental glasses that can be readily fiberized have values for Young's modulus of 19.8 million psi measured on the actual mechanically drawn fibers.

5. Attempts to obtain a consistent value for the strength of pristine fibers have not been successful as yet even though the commercial type single-hole platinum-rhodium bushings recently purchased by UARL were used.

PERSONNEL ACTIVE ON PROGRAM

Personnel active on the program throughout the fifteenth period have been James F. Bacon, principal investigator, and Francis Hale and Michael DiPerno, experimental technicians. Liaison in this quarter and throughout the program has been carried out by Peter A. Stranges of the UARL Washington office. Throughout this quarter and during the whole program the UARL personnel have reported progress to and received advice from James J. Gangler of NASA Washington Headquarters and, in the last six quarters, Michael DeCrescente of UARL.

REFERENCES

1. Morley, J. G.: Crystallization Kinetics in Some Silicate Glasses, Part I, Apparatus for the Direct Measurement of Crystal Growth at High Temperatures, Glass Technology, Vol. 6, No. 3, pp. 69-76.

2. Tiede, R. L.: Improved Apparatus for Rapid Measurement of Viscosity of Glass at High Temperature, J. Amer. Ceramic Soc., Vol. 42, pp. 537-541, (1959).

3. Tiede, R. L.: Viscometer for Measuring Glass Viscosity by Means of Flow Through an Orifice, J. Amer. Cer. Soc., Vol. 38, No. 5, pp. 183-186, May 1955.

4. Capps, Webster and Douglas H. Blackburn, N. B. S. No. 5188, The Development of Glass Fibers Having Superior Young's Moduli of Elasticity, Nat. Bur. Standards, April 1957.

5. Schile, R. D. and G. A. Rosica: Rev. Sci. Instruments 38, pp. 1103-1104, (1967).

6. Thomas, William F.: An Investigation of the Factors Likely to Affect the Strength and Properties of Glass Fibers, Physics and Chemistry of Glasses, Vol. 1, No. 1, p. 11, Feb. 1960.

Table I

New Experimental Glass Batches
Actual Ingredients in Grams

Actual Ingredient	355	356	357	358	359	360
Silica (SiO_2)	138.9	157.0	128.1	146.7	137.6	153.0
Alumina (Al_2O_3)	72.4	82.4	66.8	76.5	71.8	79.8
Magnesia (MgO)	57.9	65.2	52.7	60.4	56.8	63.1
Yttrium Oxalate	358	---	91.2	378	355	394
Zirconium Acetate	---	220	---	---	---	---
Cerium Oxalate	125.3	142.6	---	---	---	---
Rare Earth Oxalate	---	---	385	---	---	---
Zinc Carbonate	44.5	50.7	41.2	47.0	---	49.2
Lithium Carbonate	26.2	28.8	24.1	27.4	21.6	28.9
Vanadium Pentoxide	---	---	---	34.2	---	---
Zinc Tungstate	---	---	---	---	92.8	---
Cobaltous Carbonate	---	---	---	---	---	31.4

	361	362	363	364	365	366
Silica (SiO_2)	148.1	152.2	154.0	182.1	144.5	159.0
Alumina (Al_2O_3)	77.0	80.0	80.2	95.2	75.4	82.4
Magnesia (MgO)	60.9	62.9	63.5	75.2	59.5	---
Beryllium Carbonate	---	---	---	55.3	26.4	120.5
Yttrium Oxalate	382	393	396	---	372	---
Zirconium Acetate	---	---	---	---	---	268.0
Cerium Oxalate	---	---	---	164.5	130.3	143.3
Zinc Carbonate	47.5	48.8	---	58.5	---	76.5
Lithium Carbonate	27.9	28.8	29.1	34.4	27.3	---
Ferric Oxide	30.2	---	---	---	---	---
Fused Boric Acid	---	---	48.7	---	---	---
Copper Oxide	---	15.6	15.7	---	---	---

	367	368	369	370	371	372
Silica (SiO_2)	154.8	149.7	150.8	147.7	150.0	128.7
Alumina (Al_2O_3)	80.8	78.2	78.8	77.2	78.3	67.2
Magnesia (MgO)	31.9	15.5	---	---	10.3	---
Beryllium Carbonate	117.5	114	114.7	112.3	114.3	97.9
Yttrium Oxalate	396	385	389	382	387	---
Lanthanum Oxalate	---	---	---	---	---	77.3
Cerium Oxalate	93.2	90.1	90.7	88.8	90.3	---
Rare Earth Oxalate	---	---	---	---	---	388
Zinc Carbonate	---	47.9	---	47.5	32.2	82.7
Calcium Carbonate	---	---	77.2	37.7	25.5	---

Table I (Cont'd)

Actual Ingredient	373	374	375	376	377	378
Silica (SiO_2)	153.9	151.3	83.8	66.7	56.4	110.0
Alumina (Al_2O_3)	80.3	84.0	34.2	33.9	33.9	46.7
Magnesia (MgO)	---	---	35.9	35.7	35.7	49.1
Beryllium Carbonate	104.2	122.3	---	---	---	---
Yttrium Oxalate	396	416	---	---	---	---
Zirconium Acetate	---	---	---	---	---	298.0
Lanthanum Oxalate	---	---	471	474	467	---
Cerium Oxalate	92.6	---	---	---	---	---
Zinc Carbonate	---	51.8	54.9	55.6	54.8	76.5
Lithium Carbonate	29.0	30.4	48.6	49.2	48.9	67.3
Fused Boric Acid	---	---	62.1	96.0	116.2	94.2
Copper Oxide	---	11.0	---	---	---	---
Calcium Carbonate	39.4	---	67.2	66.5	66.5	91.8

	379	380	381	382	383	384
Silica (SiO_2)	99.9	91.5	111.2	107.2	111.2	82.2
Alumina (Al_2O_3)	21.2	---	23.4	22.8	23.6	17.5
Magnesia (MgO)	44.6	40.8	49.7	47.9	49.7	36.7
Zirconium Acetate	272	248	303	291	302	---
Lanthanum Oxalate	146	278	---	---	---	---
Zinc Carbonate	69.6	63.3	77.1	74.2	77.2	57.0
Lithium Carbonate	61.2	56.1	62.1	65.7	68.4	50.4
Fused Boric Acid	85.8	78.2	95.5	92.2	95.5	70.3
Calcium Carbonate	83.0	74.8	92.5	89.2	92.7	68.5
Copper Oxide	---	---	18.5	---	---	---
Titanium Oxide (not rutile)	---	---	---	---	18.6	---
Beryllium Carbonate	---	---	---	---	---	17.4
Ferric Oxide	---	---	---	35.7	---	---
Rare Earth Oxalate	---	---	---	---	---	483

	385	386	387	388	389	390
Silica (SiO_2)	9.6	8.3	53.1	87.3	96.7	76.9
Alumina (Al_2O_3)	338.9	263.5	---	---	39.4	39.2
Lithium Carbonate	37.8	32.4	52.1	53.5	57.1	56.7
Calcium Carbonate	188.3	145.8	265.0	72.7	77.2	76.5
Zinc Carbonate	32.2	27.6	44.4	---	64.4	64.2
Magnesia (MgO)	10.3	8.9	7.2	29.3	41.4	41.3
Fused Boric Acid	---	---	63.1	74.7	71.6	110.9
Lanthanum Oxalate	---	154.7	248.7	---	---	---
Titanium Oxide (not rutile)	---	---	14.1	19.4	---	---
Beryllium Carbonate	---	---	306.5	84.2	---	---
Ferric Oxide	---	35.2	---	---	---	---
Rare Earth Oxalate	---	---	---	513	---	---
Yttrium Oxalate	---	---	---	---	466	463

Table I (Cont'd)

Actual Ingredient	391	392	393	394	395	396
Silica (SiO_2)	65.1	81.0	79.1	87.6	72.3	194
Alumina (Al_2O_3)	39.0	37.4	61.0	67.6	61.4	108.7
Lithium Carbonate	50.2	45.2	44.2	39.2	73.0	52.8
Calcium Carbonate	76.3	61.2	---	---	---	---
Zinc Carbonate	63.9	76.8	75.1	58.4	75.2	---
Magnesia (MgO)	41.0	37.0	48.2	80.2	48.6	43.3
Fused Boric Acid	133.7	83.1	81.5	90.0	74.1	---
Zirconium Acetate	---	79.9	97.5	---	196.0	351
Copper Oxide	---	---	---	10.3	---	---
Yttrium Oxalate	462	443	443	400	362	433

	397	398	399	400	401	402
Silica (SiO_2)	192.3	92.5	90.8	94.9	91.4	90.2
Alumina (Al_2O_3)	203.8	50.3	48.9	---	49.5	49.0
Lithium Carbonate	61.6	45.2	30.7	46.5	22.3	22.1
Calcium Carbonate	---	80.0	60.2	94.8	72.7	54.2
Zinc Carbonate	80.5	---	54.1	47.5	---	---
Magnesia (MgO)	---	31.6	38.7	40.7	48.9	48.4
Fused Boric Acid	---	106.5	103.6	109.6	104.9	103.9
Copper Oxide	---	---	---	---	9.65	9.6
Titanium Oxide (not rutile)	---	---	---	---	---	14.4
Yttrium Oxalate	---	523	507	536	512.5	506

	403	404	405	406
Silica (SiO_2)	87.3	88.1	153.3	124.3
Alumina (Al_2O_3)	47.4	47.8	73.3	59.9
Lithium Carbonate	21.4	21.4	2.72	2.22
Calcium Carbonate	34.8	37.2	---	---
Magnesia (MgO)	46.7	47.2	---	---
Fused Boric Acid	100	57.1	---	---
Lanthanum Oxalate	---	---	---	648.5
Copper Oxide	9.2	9.3	---	---
Titanium Oxide (not rutile)	13.9	14.1	---	---
Beryllium Carbonate	---	17.8	73.5	60.2
Ferric Oxide	27.8	28.1	---	---
Yttrium Oxalate	490	495	682	---

Table II

Composition in Mol % of Borate-Series Glasses

Actual Ingredient	290	291	299	300	375
SiO_2	25	25	25	25	25
Al_2O_3	8	12	8	--	6
Li_2O	15	12	15	15	12
CaO	--	--	15	15	12
ZnO	15	12	--	15	8
MgO	15	12	15	15	16
B_2O_3	15	15	15	15	9
Y_2O_3	7	12	--	--	--
La_2O_3	--	--	7	--	12
Young's Modulus (10^6 psi)	14.5	15.67	14.57	14.45	16.58
Density (gms/cm^3)	3.24	3.32	3.19	2.89	3.68
Specific Modulus (10^7 in.)	12.3	13.1	12.7	13.9	12.4
Molal Sum	72.16	82.98	75.36	56.6	89.8

	376	377	378	379	380
SiO_2	20	17	24	24	24
Al_2O_3	6	6	6	3	--
Li_2O	12	12	12	12	12
CaO	12	12	12	12	12
ZnO	8	8	8	8	8
MgO	16	16	16	16	16
B_2O_3	14	17	10	10	10
La_2O_3	12	12	--	3	6
ZrO_2	--	--	12	12	12
Young's Modulus (10^6 psi)	15.80	15.02	14.4	17.3	15.7
Density (gms/cm^3)	3.68	3.61	3.17	3.14	--
Specific Modulus (10^7 in.)	11.8	11.5	12.5	15.2	--
Molal Sum	90.3	90.5	65.6	72.3	79.0

Table II (Cont'd)

Actual Ingredient	381	382	383	384	387
SiO_2	24	24	24	24	10
Al_2O_3	3	3	3	3	--
Li_2O	12	12	12	12	8
CaO	12	12	12	12	30
ZnO	8	8	8	8	4
MgO	16	16	16	16	2
B_2O_3	10	10	10	10	6
La_2O_3	--	--	--	--	4
ZrO_2	12	12	12	--	--
CuO	3	--	--	--	--
TiO_2	--	--	3	--	2
BeO	--	--	--	3	34
Re_2O_3 (rare earth oxide)	--	--	--	12	--
Fe_2O_3	--	3	--	--	--
Young's Modulus (10^6 psi)	15.87	17.7	22.75	18.62	17.85
Density (gms/cm^3)	2.96	3.01	3.14	3.89	3.28
Specific Modulus (10^7 in.)	14.9	16.3	20.0	13.2	15.0
Molal Sum	64.9	67.3	64.9	87.9	56.6

	388	389	390	391	392
SiO_2	24	25	20	17	22
Al_2O_3	--	6	6	6	6
Li_2O	12	12	12	12	10
CaO	12	12	12	12	10
ZnO	--	8	8	8	10
MgO	12	16	16	16	15
B_2O_3	10	9	14	17	11
Y_2O_3	--	12	12	12	12
ZrO_2	--	--	--	--	4
TiO_2	4	--	--	--	--
BeO	14	--	--	--	--
Re_2O_3 (rare earth oxide)	12	--	--	--	--
Young's Modulus (10^6 psi)	17.28	17.2	16.80	17.38	16.24
Density (gms/cm^3)	3.58	3.45	3.35	3.31	--
Specific Modulus (10^7 in.)	13.4	13.8	13.9	14.6	--
Molal Sum	82.6	77.8	78.2	78.5	81.8

Table II (Cont'd)

Actual Ingredient	393	394	395	398	399	400
SiO_2	22	22	20	25	25	25
Al_2O_3	10	10	10	8	8	--
Li_2O	10	8	10	10	7	10
CaO	--	--	--	13	10	15
ZnO	10	7	10	--	6	6
MgO	20	30	20	16	16	16
B_2O_3	11	11	10	14	14	14
Y_2O_3	12	10	10	14	14	14
ZrO_2	5	--	10	--	--	--
CuO	--	2	--	--	--	--
Young's Modulus (10^6 psi)	16.46	16.59	16.00	16.30	16.89	--
Molal Sum	83.5	75.4	83.3	81.3	83.6	79.1

Table III

Summary of All Values for Young's Modulus Measured on Circular Rods Formed Directly from Melt

Glass Number	Density lbs/in³	Young's Modulus millions psi	Specific Modulus 10^7 inches	Glass Number	Density lbs/in³	Young's Modulus millions psi	Specific Modulus 10^7 inches	Glass Number	Density lbs/in³	Young's Modulus millions psi	Specific Modulus 10^7 inches
40-3[3]	0.1067	15.5	14.5	135[3]	0.0946	14.3	15.1	234[3]	0.1338	18.1	13.5
62-3[3]	0.0989	14.2	16.2	136[3]	0.1012	14.4	14.2	235[3]	0.1203	17.4	14.4
67-3[3]	0.0957	14.4	15.0	137[3]	0.1113	13.3	12.0	236[3]	0.1249	17.8	14.3
68-3[3]	0.0950	14.1	14.8	138[3]	0.1282	15.3	12.0	237[3]	0.1203	18.3	15.2
69-3[3]	0.0935	14.2	15.2	140[3]	0.1329	15.6	11.7	238[3]	0.1098	16.6	15.1
72-2[3]	0.1043	14.0	13.4	151	0.1175	16.9	14.4	247[1]	0.1078	15.1	14.0
83[2]	0.1026	16.0	15.6	155[3]	0.1282	15.7	12.2	248[1]	0.1118	15.7	14.0
96	0.1071	16.33	15.24	157[3]	0.0972	13.3	13.7	249[1]	0.1087	15.9	14.6
97	0.1027	15.5	15.1	159[3]	0.1163	16.2	13.9	250[1]	0.1561	14.8	9.47
99[1]	0.1152	10.5	9.12	166[3]	0.0946	12.5	13.2	251[1]	0.1108	15.9	14.3
102[1]	0.1050	15.0	14.3	174[3]	0.1253	16.5	13.2	252[1]	0.1108	14.9	13.5
108[1]	0.1133	14.8	13.1	175[3]	0.1152	16.1	14.0	253[1]	0.1172	12.3	10.5
110[3]	0.0939	14.6	15.5	176[3]	0.1137	15.2	13.4	256[1]	0.1296	17.9	13.8
114[3]	0.1163	16.7	14.4	179[3]	0.1553	14.9	9.6	257[1]	0.1347	18.4	13.7
125[3]	0.1000	16.1	16.1	194	0.1618	14.7	9.2	258	0.0978	13.5	13.7
126[3]	0.1250	16.8	13.4	219	0.1072	14.8	13.8	259	0.1043	13.2	12.6
127[3]	0.1173	16.1	13.7	222	0.1620	14.8	9.1	263[3]	0.1447	14.5	10.0
129[3]	0.1193	16.5	13.8	231[3]	0.1240	18.05	14.55	265[1]	0.1439	16.3	11.3
131[3]	0.1132	14.0	13.5	232[3]	0.1297	18.1	13.9	266[1]	0.1153	16.7	14.5
134[3]	0.1107	15.4	13.9	233[3]	0.1093	15.86	14.5	267[1,2]	0.0976	15.3	15.7

Table III (Cont'd)

Glass Number	Density lbs/in^3	Young's Modulus millions psi	Specific Modulus 10^7 inches	Glass Number	Density lbs/in^3	Young's Modulus millions psi	Specific Modulus 10^7 inches	Glass Number	Density lbs/in^3	Young's Modulus millions psi	Specific Modulus 10^7 inches
268[1]	0.1155	16.9	14.6	285[1]	0.1322	15.1	11.4	310[1,2]	0.1327	16.7	12.6
269[1]	0.1242	17.2	13.8	286[1]	0.1368	15.6	11.4	311[1,2]	0.1337	15.9	11.1
270[1]	0.1275	20.3	15.9	287[1]	0.1308	15.1	11.5	312[1,2]	0.1183	16.5	14.0
273-1[1,2]	0.0988	18.4	18.6	288[1]	0.1303	14.3	11.0	314[1]	0.1342	17.0	12.6
273-2[1,2]	0.0988	17.2	17.4	289[1]	0.1407	15.0	10.7	315[1,2]	0.1293	16.6	12.8
274[1,2]	0.1077	17.2	15.9	290[1]	0.1172	14.5	12.3	316[1,2]	0.1373	16.5	12.0
275-1[1,2]	0.1318	16.7	12.7	291[1]	0.1200	15.7	13.1	317[1,2]	0.1375	16.3	11.9
275-2[1,2]	0.1318	16.8	12.7	292[1]	0.1322	15.4	11.6	318[1,2]	0.0978	16.0	16.4
276[1,2]	0.1227	15.8	12.9	293[1]	0.1187	16.0	13.5	319	0.1310	17.9	13.7
277[1,2]	0.1413	17.9	12.6	294[1]	0.1217	17.6	14.4	320	0.1057	16.0	15.1
278	0.0942	13.3	13.6	295[1]	0.1152	15.2	13.2	321[3]	0.1313	18.7	14.2
278[4]	0.0942	15.2	16.1	296[1]	0.1187	16.5	13.9	322[1,2]	0.1080	16.9	15.65
279	0.0972	12.4	12.7	297[1]	0.1278	17.1	13.4	323[1,2]	0.0999	18.4	18.4
280	0.0742	5.56	7.5	299[1]	0.1150	14.6	12.7	324[1,2]	0.1072	17.8	16.6
280[4]	0.0742	6.23	8.40	300[1]	0.1042	14.5	13.9	325[1,2]	0.1280	20.2	15.8
281	0.0871	6.77	7.77	302[1]	0.1358	17.2	12.6	326[1,2]	0.1115	17.0	15.3
282	0.0798	4.80	6.00	304[3]	0.1307	19.2	14.7	327[1]	0.1330	18.4	13.8
282[4]	0.0798	6.22	7.80	305[3]	0.1320	17.7	13.4	328[1]	0.1578	18.5	11.7
283[1]	0.1313	15.5	11.8	306[3]	0.1322	18.9	14.3	329[1]	0.1095	20.7	18.9
284[1]	0.1200	14.9	12.4	309[1,2]	0.1296	16.9	13.0	330[1,2]	0.1462	18.6	12.7

Table III (Cont'd)

Glass Number	Density lbs/in^3	Young's Modulus millions psi	Specific Modulus 10^7 inches
331[1,2]	0.1322	20.9	15.8
332[1]	0.1528	17.3	11.3
333[1]	0.1338	18.9	14.1
334[1]	0.1422	17.5	12.3
335[1,2]	0.1392	19.0	13.6
336[1,2]	0.1265	21.0	16.6
337[1]	0.1423	20.9	14.7
338[1]	0.1508	----	----
339[1,2]	0.1500	19.4	13.0
340[1,2]	0.1283	20.9	16.3
341[1,2]	0.1413	18.9	13.4
342[1,2]	0.1322	----	----
343[1,2]	0.1383	19.4	14.0
344[2,3]	0.1225	20.3	16.8
345[2,3]	0.1208	21.1	17.45
346[1,2]	0.1282	17.66	13.8
347[1,2]	0.1312	21.6	16.4
348[1,2]	0.1317	17.7	13.4
349[1,2]	0.1273	16.8	13.2
350[1,2]	0.1006	19.8	19.7

Glass Number	Density lbs/in^3	Young's Modulus millions psi	Specific Modulus 10^7 inches
351[1,2]	0.1003	17.0	17.0
352[1,2]	0.1368	20.0	14.6
353[1,2]	0.1413	19.4	13.7
354[1,2]	0.1288	18.4	14.3
355[3]	0.1365	18.1	13.2
356[3]	0.1210	13.9	11.5
357[3]	0.1222	17.6	14.4
358[3]	0.1257	13.1	10.4
359[3]	0.1337	17.6	13.2
360[3]	0.1269	18.5	14.6
361[3]	0.1260	18.6	14.8
362[3]	0.1260	18.0	14.3
96-2	0.1057	15.4	14.6
331A[1,2]	0.1310	20.07	15.35
SFS1	----	6.98	----
SF6	0.1868	6.91	3.69
LaSF3	0.177	13.3	7.52
LaSF6	0.2207	17.4	7.88

Glass Number	Density lbs/in^3	Young's Modulus millions psi	Specific Modulus 10^7 inches
X-2285	0.0899	14.95	16.65
SiO_2	0.079	10.5	13.3
"E"	0.092	10.5	11.4
"S"	0.090	12.6	14.0
Steel	0.280	29	10.3
Al_2O_3	0.114	25	21.9
ZrO_2	0.175	50	28.6
BN	0.069	13	18.8
MO	0.369	52	14.1

[1]Invert Analog Glasses
[2]Contains BeO
[3]Cordierite Base Glasses
[4]Heat treated two phase

Table IV

Summary Extended All Values for Young's Modulus Measured On Circular Rods Formed Directly From Melt - Melts 360 et. seq.

Glass No.	Density gms/cm^3	Density lbs/in^3	Young's Modulus millions psi	Specific Modulus 10^7 inches
356A[1,3]	3.3158	0.1193	13.9	11.63
360[1,3]	3.5183	0.1269	18.5	14.6
361[1,3]	3.4989	0.1260	18.6	14.8
362[1]	3.4997	0.1260	18.0	14.3
363[1,3]	3.5680	0.1289	19.26	14.9
364[1,2]	3.0985	0.1120	16.70	14.9
365[1,2,3]	3.5453	0.1281	19.04	14.9
366[1,2,3]	3.4697	0.1255	16.19	12.9
367[1,2,3]	3.5310	0.1277	19.03	14.9
368[1,2,3]	3.6229	0.1320	19.08	14.4
369[1,2,3]	3.5272	0.1277	17.78	13.9
370[1,2,3]	3.6285	0.1313	18.59	14.15
371[1,2,3]	3.5664	0.1289	18.54	14.4
372[1,2,3]	4.0747	0.1473	17.34	11.8
373[1,2,3]	3.4937	0.1262	19.00	15.05
373A[1,2,3]	3.4937	0.1262	22.0	17.35
374[1,2,3]	3.4276	0.1238	19.00	15.45
374A[1,2,3]	3.4276	0.1238	19.15	15.5
375[1]	3.6819	0.1333	16.58	12.42
375A[1]	3.6819	0.1333	15.73	11.8
376[1]	3.6820	0.1334	15.80	11.85
376R[1]	3.6820	0.1334	15.75	11.79
377[1]	3.6108	0.1304	15.62	11.96
377R[1]	3.6108	0.1304	15.02	11.53
378[1]	3.2971	0.1192		

Table IV (Cont'd)

Glass No.	Density gms/cm^3	Density lbs/in^3	Young's Modulus millions psi	Specific Modulus 10^7 inches
378A[1]	3.1701	0.1147	14.4	12.55
379[1]	3.1448	0.1137	17.3	15.22
380[1]			15.7	
381[1]	2.9591	0.1063	15.87	14.9
382[1]	3.0054	0.1082	17.7	16.32
383[1]	3.1418	0.1136	22.75	20.02
384[1,2]	3.8927	0.1407	18.62	13.23
385	2.8006	0.1011		
386	3.3705	0.1218		
387[2]	3.2777	0.1183	17.85	15.08
388[2]	3.5767	0.1293	17.28	13.38
389[1]	3.4540	0.1247	17.2	13.80
390B[1]	3.3462	0.1210	16.80	13.88
391A[1]	3.3062	0.1193	17.38	14.57
392			16.24	
393			16.46	
394			16.59	
395			16.00	
396			15.15	
398			16.30	
399			16.89	

[1] Invert Analog Glasses
[2] Contains BeO
[3] Cordierite Base Glasses

Table V

Best Glasses To Date Obtained In Cordierite Rare-Earth Systems

	Glass Number	Young's Modulus (millions psi)	Specific Modulus (millions-inches)
No BeO			
	125	16.1	161
	337	20.9	147
	363	19.3	150
With BeO			
	345	21.1	174
	344	20.3	168
	323	18.4	184
To Be Compared With			
Owens Corning	x-2285	14.95	167
	Steel	29	103
	Molybdenum	52	141

Table VI

Best Glasses To Date Obtained In "Invert" Analog Systems

	Glass Number	Young's Modulus (millions psi)	Specific Modulus (millions-inches)
No BeO			
	383	22.75	200
	329	20.7	189
With BeO	373	22.00	173
	350	19.8	197
	331	20.9	158
To Be Compared With			
Owens Corning	x-2285	14.95	167
	Steel	29	103
	Molybdenum	52	141

Table VII

Liquidus Temperature and Working Characteristics of Recent Experimental Glasses

Glass No.	Liquidus Temp. °C	Temperature at Which Viscosity Is Estimated to Be: 100 poises	1000 poises	Rate of Crystal Growth 50°C below Liquidus Temperature
333	1510	1490	1440	few isolated crystals
339	1520	1540	1430	none
340	1507	1520	1400	none
341	1438	1390	1515	none
342	1470	1350	1485	few isolated crystals
343	1410	1200	1420	none
347	1510	1406	1506	not apparent
348	1450	1310	1448	none
349	1480	1320	1450	none
350	1510	1422	1490	very rapid
351	1450	1331	1435	very slow
352	1435	1340	1422	moderate
353	1510	1315	1406	extremely rapid
354	1464	1290	1414	moderate
359	1490	1380	1500	few isolated crystals
367	1460	too opaque	too opaque	a very few isolated
368	1440	too opaque	too opaque	none
370	1500	1290	1460	none
371	1498	1290	1372	a very few isolated
372	1440	1300	1420	few isolated crystals
373	1510	1368 (many crystals)	1435	none
374	1456	1300	1481	only micro-crystals
375	1347	1256	1332	many micro-crystals
376	1122	951	1150	none
377	1156	933	1222	none

Table VIII

First Experiments on Measuring Strength of "E" Glass Fibers Formed By Pulling From a Commercial-Type Single Hole Platinum-Rhodium Bushing

Diameter (mils)	Strength (psi)	Diameter (mils)	Strength (psi)	Diameter (mils)	Strength (psi)
0.563	147,000	0.557	122,500	0.719	219,000
0.581	139,000	0.563	190,000	0.759	149,000
0.581	112,000	0.471	177,000	0.692	138,000
0.581	66,600	0.471	171,000	0.685	128,000
0.633	123,000	0.493	167,000	0.658	113,000
0.664	223,000	0.713	135,000	0.655	239,000
0.652	152,000	0.713	124,000	0.569	110,000
0.630	129,000	0.737	124,000	0.563	186,000
0.584	95,400	0.594	183,000	0.566	144,000
0.566	119,000	0.600	191,000	0.572	172,000
0.536	150,000	0.441	493,000	0.560	211,000
0.529	160,400	0.597	122,000	0.575	182,000
0.523	236,000	0.523	210,000	0.621	207,000
0.496	106,000	0.505	127,000	0.581	237,000
0.526	101,000	0.508	190,000	0.710	187,000
0.505	209,000	0.542	177,000	0.786	218,000
0.493	243,000	0.517	194,000	0.655	124,000
0.505	116,000	0.502	228,000	0.633	126,000
0.523	231,000	0.517	236,000	0.676	104,000
0.502	150,000	0.505	232,000	0.692	156,000
0.539	227,000	0.551	162,000	0.664	119,000
0.517	205,000	0.575	110,000	0.670	151,000
0.419	136,000	0.578	151,000	0.588	161,000
0.438	184,000	0.569	148,000	0.591	180,000
0.444	199,000	0.591	330,000	0.578	166,000
0.410	150,000	0.597	122,000	0.581	108,500
0.413	247,000	0.578	117,000	0.560	116,500
0.529	195,000	0.609	174,000	0.520	77,600
0.542	205,000	0.581	270,000	0.542	177,000
0.557	122,000	0.618	103,000	0.532	163,000
0.567	117,000	0.627	140,000	0.520	67,300
0.530	88,000	0.734	164,000	0.539	160,000
0.526	111,000	0.750	195,000	0.496	240,000

H910373-15

FIG. 1

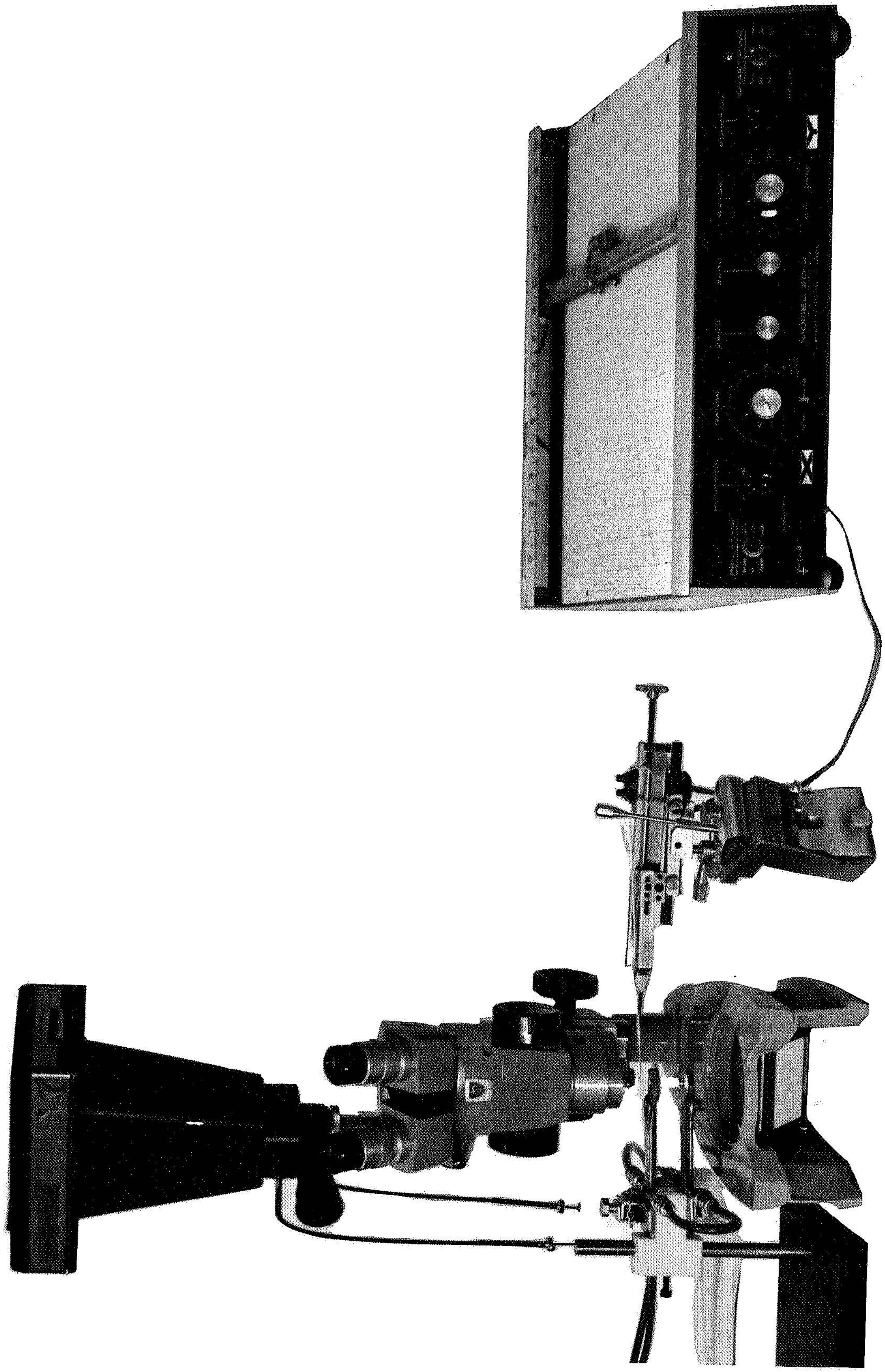

CLOSE-UP OF MICRO-FURNACE, HEAT SHIELDS REMOVED

H910373-15

FIG. 2

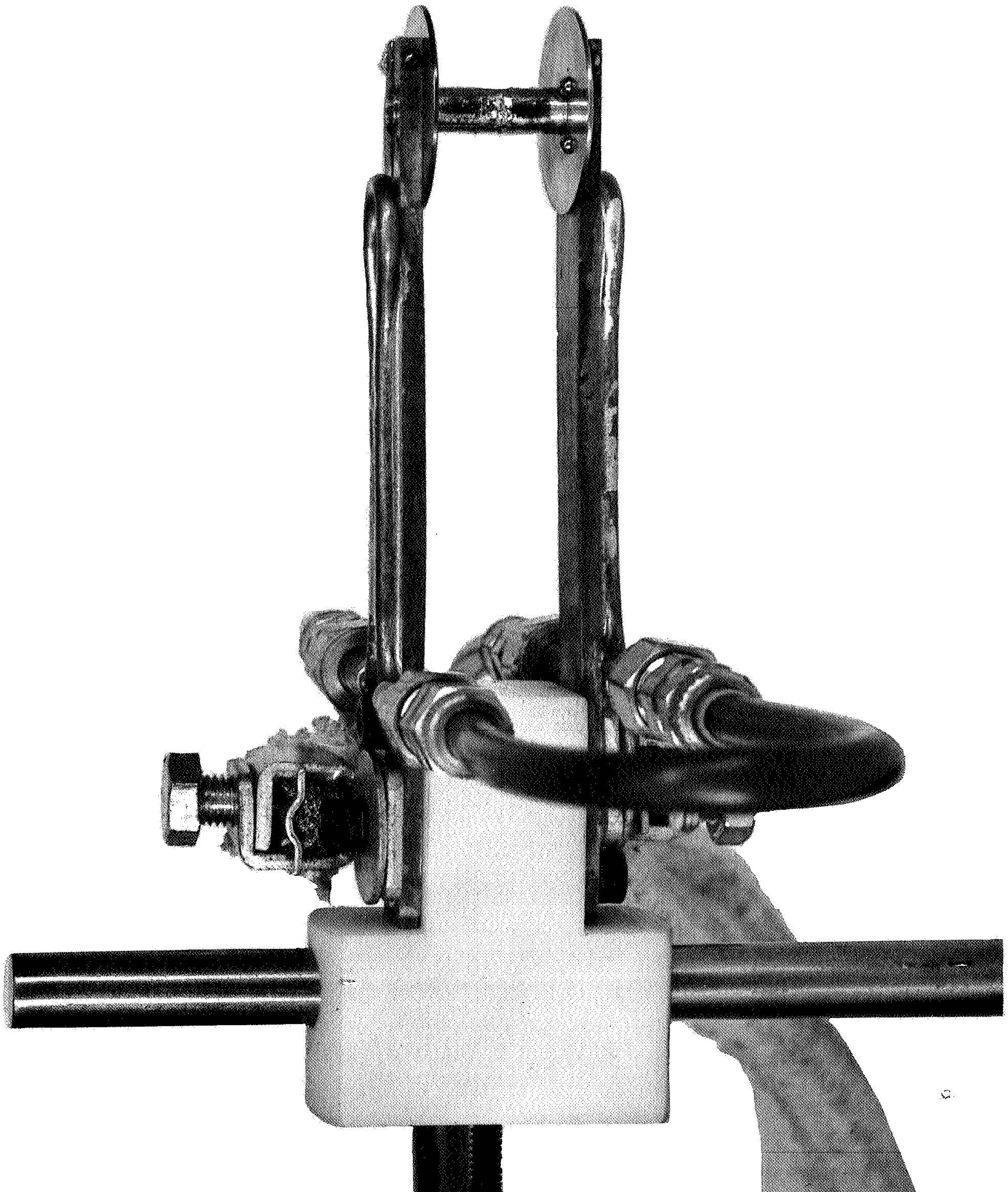

MICRO-FURNACE AND ALL ASSOCIATED EQUIPMENT

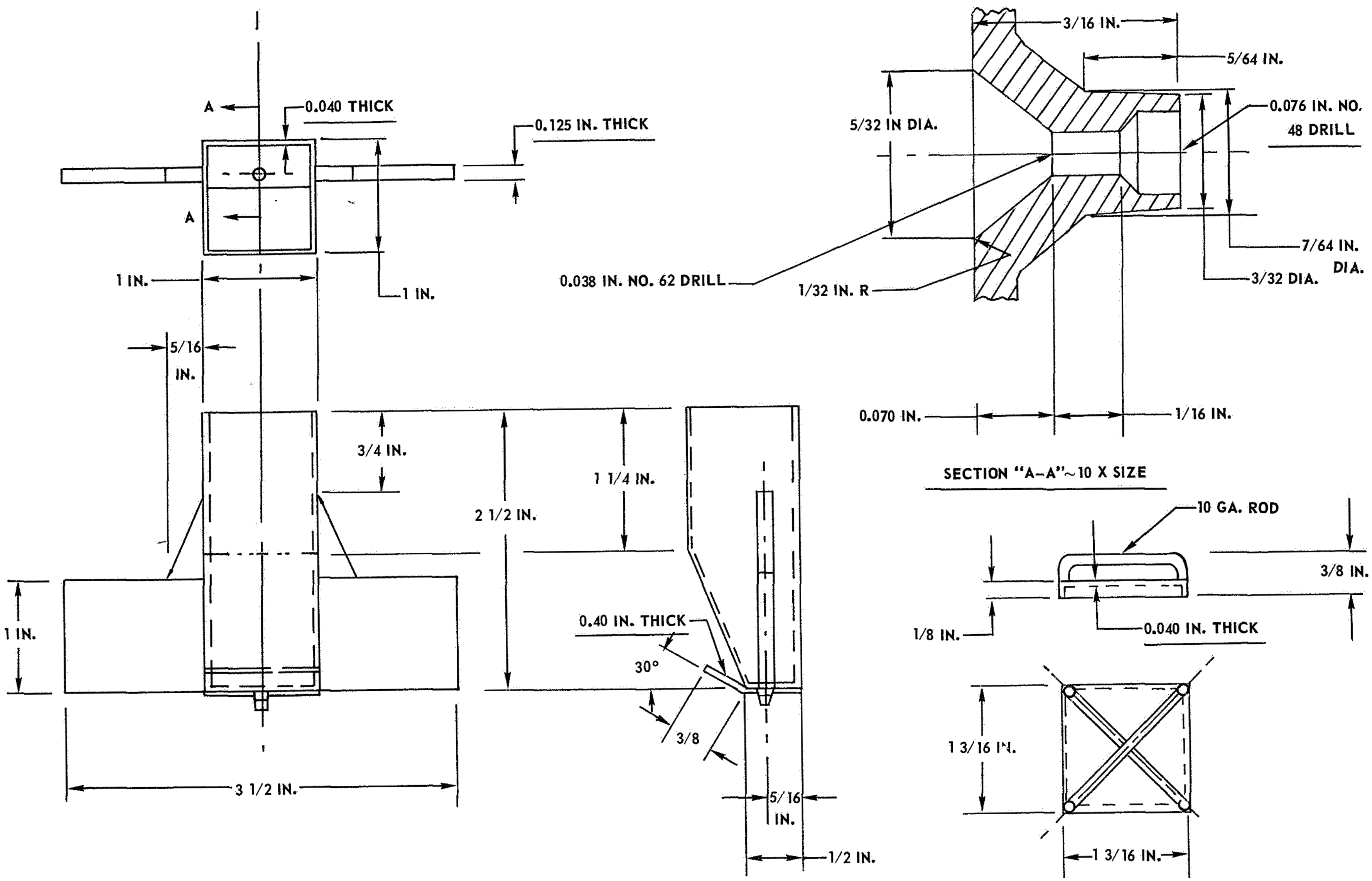

FIG. 3

UARL DESIGN FOR SINGLE-HOLE BUSHING PATTERNED AFTER THOSE OF TIEDE (REF. 32) AND NAT. BUR. STANDARDS (REF. 33)

FIG. 4

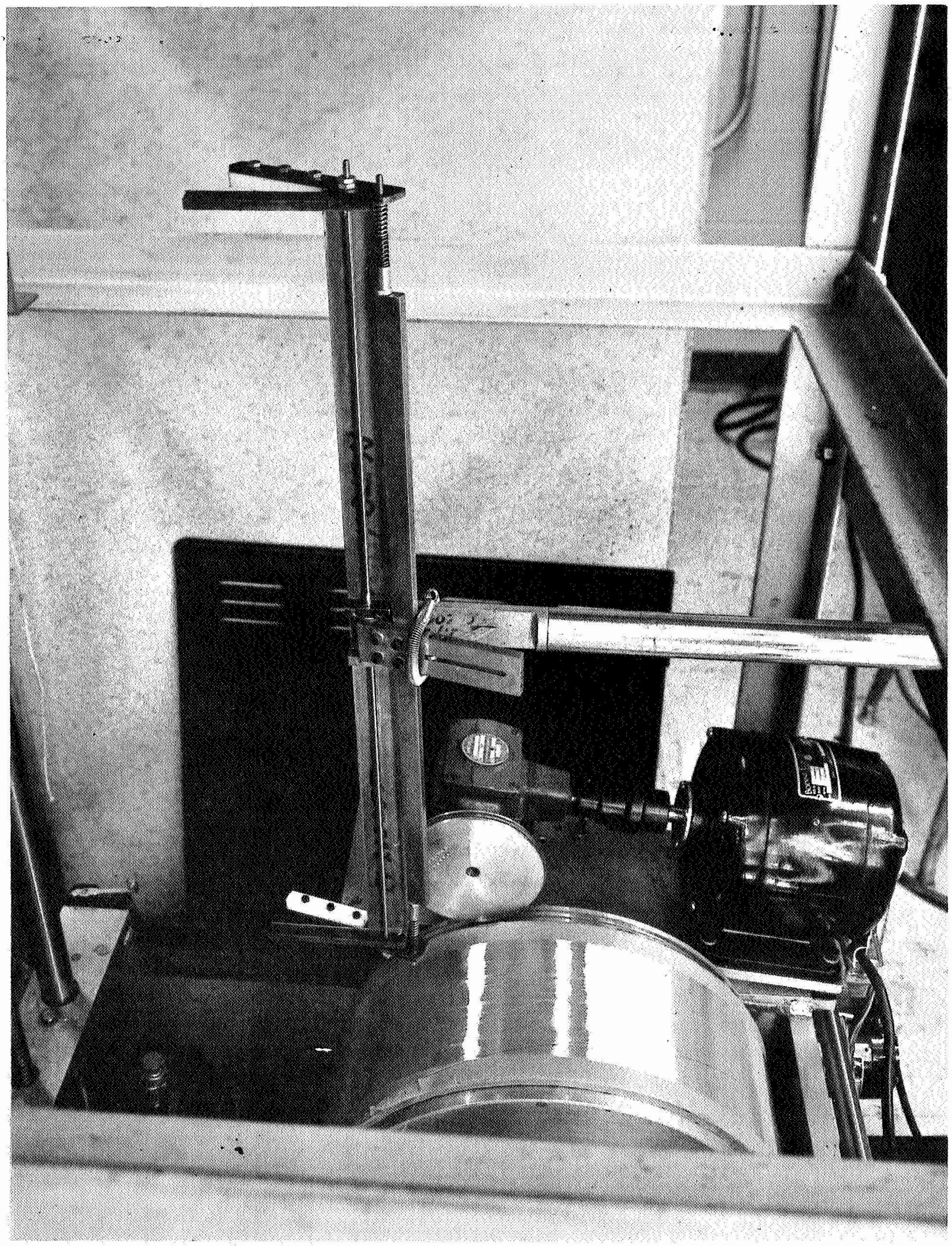

FIBER CAPTURE DEVICE

FIG. 5

TENSILE TESTER

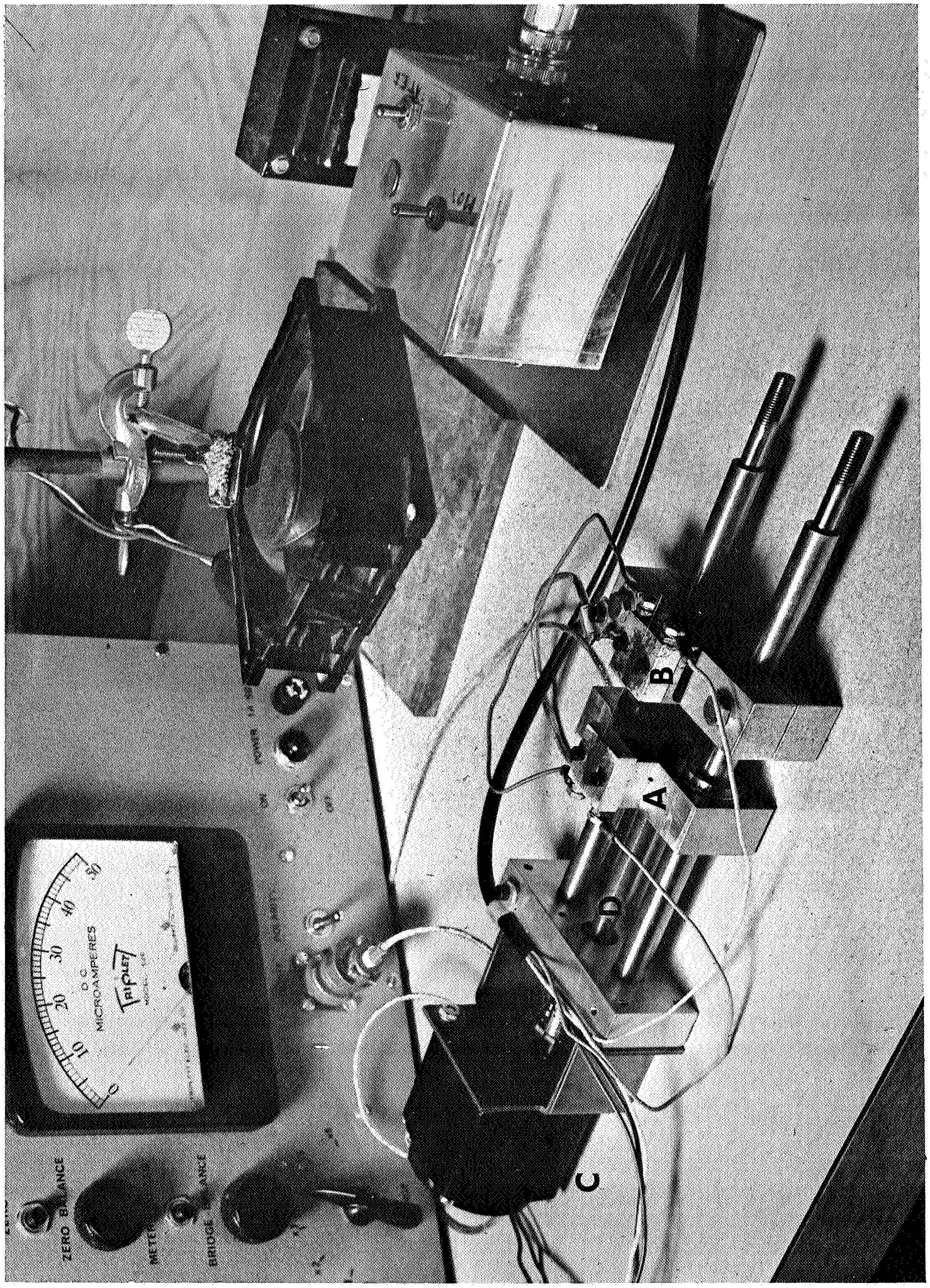

FIG. 6

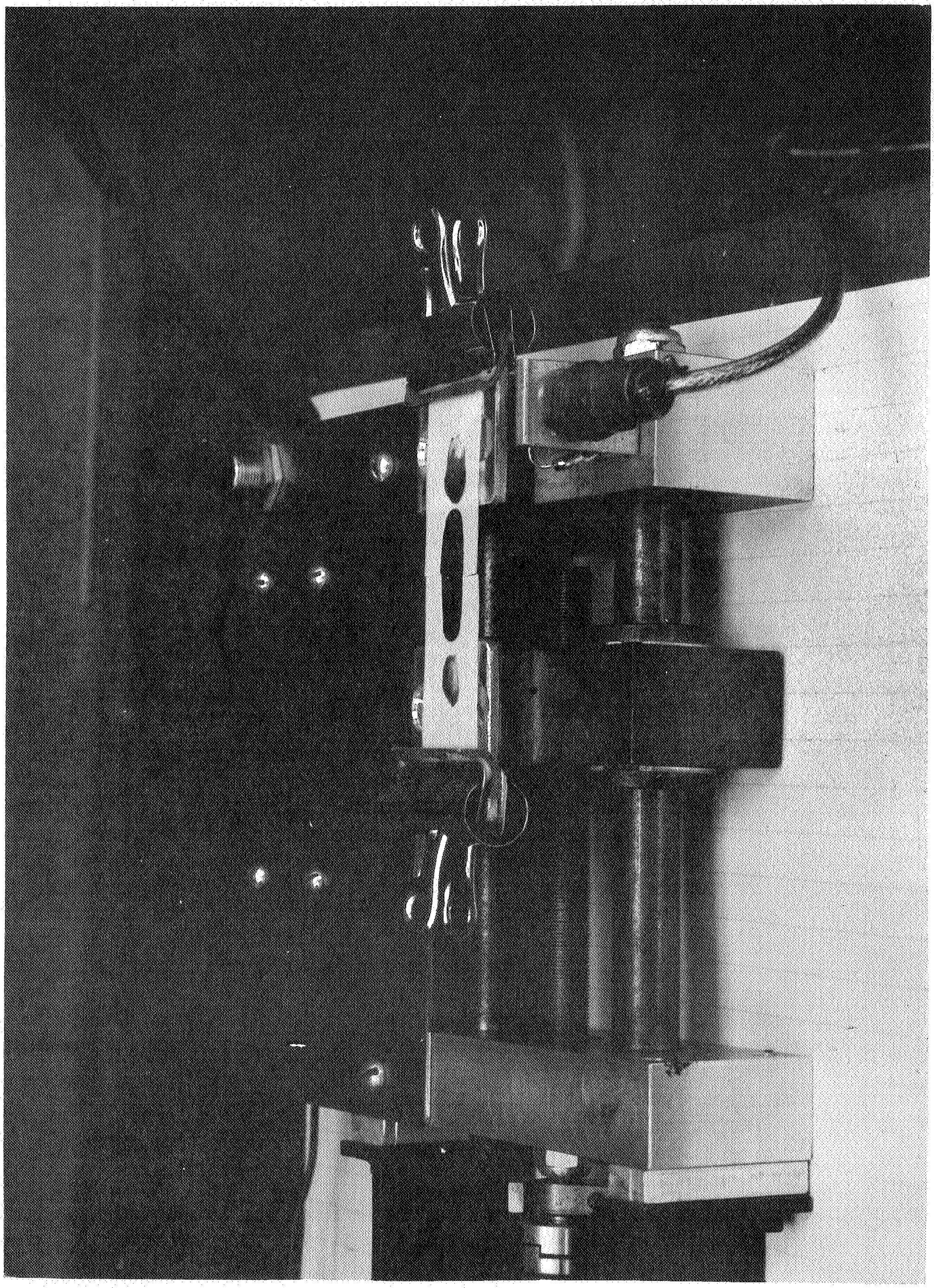

PAPER TAB MOUNTING SYSTEM